designs

MDPI

Article

Secured Multi-Dimensional Robust Optimization Model for Remotely Piloted Aircraft System (RPAS) Delivery Network Based on the SORA Standard

Armin Mahmoodi [1], Leila Hashemi [1], Jeremy Laliberté [1,*] and Richard C. Millar [2]

[1] Department of Mechanical and Aerospace Engineering, Carleton University, Ottawa, ON K1S 5B6, Canada; arminmahmoodi@cmail.carleton.ca (A.M.); seyedehleilahashemi@cmail.carleton.ca (L.H.)
[2] Department of Engineering Management and Systems Engineering, The George Washington University, Washington, DC 20052, USA; rcmillar@gwu.edu
* Correspondence: jeremy.laliberte@cunet.carleton.ca

Abstract: The range of applications of RPAs in various industries indicates that their increased usage could reduce operational costs and time. Remotely piloted aircraft systems (RPASs) can be deployed quickly and effectively in numerous distribution systems and even during a crisis by eliminating existing problems in ground transport due to their structure and flexibility. Moreover, they can also be useful in data collection in damaged areas by correctly defining the condition of flight trajectories. Hence, defining a framework and model for better regulation and management of RPAS-based systems appears necessary; a model that could accurately predict what will happen in practice through the real simulation of the circumstances of distribution systems. Therefore, this study attempts to propose a multi-objective location-routing optimization model by specifying time window constraints, simultaneous pick-up and delivery demands, and the possibility of recharging the used batteries to reduce, firstly, transport costs, secondly, delivery times, and thirdly, estimated risks. Furthermore, the delivery time of the model has been optimized to increase its accuracy based on the uncertain conditions of possible traffic scenarios. It is also imperative to note that the assessment of risk indicators was conducted based on the Specific Operations Risk Assessment (SORA) standard to define the third objective function, which was conducted in a few previous studies. Finally, it shows how the developed NSGA-II algorithm in this study performed successfully and reduced the objective function by 31%. Comparing the obtained results using an NSGA-II meta-heuristic approach, through the rigorous method GAMS, indicates that the results are valid and reliable.

Keywords: remotely piloted aircraft system (RPAS); multi-objective optimization; NSGAII algorithm; location-routing problem; robust optimization; SORA standard

Citation: Mahmoodi, A.; Hashemi, L.; Laliberté, J.; Millar, R.C. Secured Multi-Dimensional Robust Optimization Model for Remotely Piloted Aircraft System (RPAS) Delivery Network Based on the SORA Standard. *Designs* **2022**, *6*, 55. https://doi.org/10.3390/designs6030055

Academic Editor: Ruxandra Botez

Received: 25 April 2022
Accepted: 6 June 2022
Published: 15 June 2022

1. Introduction

Due to the growing population of industrial cities, conventional and land transport systems face both time and cost constraints in meeting the increasing demand of their customers. In populated cities, the saturation of land transport vehicles has led big companies to consider replacing them with RPAS-based distribution systems to reduce costs [1]. As a result of this replacement, RPAS-based online companies grow, which not only leads to more efficient, reliable, and capable RPASs but also increases the market for product manufacture and delivery due to an increase in transport companies [2]. Often known as smart vehicles, RPASs can be lightweight, small, cost-effective, and increasingly capable of automatic operation [3]. Information and communications technology (ICT) is considered to be the main activity center for RPASs. As a result of this technology, RPASs can receive and collect data promptly and act in the defined timeframe with integrated and cooperative performance in a supply chain, things that are close to the concept of "IoT" (Internet of Things). In an IoT setting, interrelated components transfer data over the network, very similar to the role of RPASs in gathering data. Therefore, they are applicable in any IoT-based operation [4], such as rescue missions and monitoring [5], agriculture [6] weather forecasts, and most importantly, transport/location [7–9].

Although RPASs are increasingly popular in numerous areas of application in industries and universities [10,11], nonetheless, challenges such as heavy air traffic in urban and non-urban permitted flying areas, flight time constraints, batteries or loading limits, and unexpected weather conditions necessitate the design of a model for optimal routing throughout the supply chain of distribution.

In fact, the challenge of most RPAS-based distribution network optimization models is finding the best route when environmental circumstances of selected routes, including ground and weather factors, are predictable and can be determined with high accuracy. This optimization is only possible through the correct transfer of flight data, along with the reliable and lasting communication of RPASs with ground stations or with other RPASs. This matter, nevertheless, requires the identification of its potential risks such as loss of in-flight communication, and most importantly, probable occurrences during the transport since there is a probability of RPASs colliding with the ground and hitting people or other vehicles, or any obstacle in general as the operation of RPASs expands in low-altitude and/or uncontrolled airspace classes [12].

Concerning this, some researchers have focused on minimizing transport costs and time in RPASs-based route planning or maximizing supply chain demands under certain and uncertain circumstances [2,13,14]. Most have used classic Vehicle Routing Problem (VRPD) models to simulate real situations, whose distinctions have been examined based on their scales. Constraints such as on-demand delivery or pick-up, specific time constraints based on soft and hard time windows, the possibility of recharging RPAS batteries in DCs, loading-related constraints, not only stress the diversity of studies conducted but also show to what extent potential risks prevail in a location-routing network.

This study attempts not only to cover all aspects analyzed in past studies, but also to assess identified risks, both in the air and on the ground, on selected trajectories based on the SORA standard [15] and reduce them by proposing a novel and developed model. The planning for flight trajectories begins from the starting points (facility locations), splits into DCs, and ends at the demand points. The proposed model is a multi-dimensional and multi-echelon RPAS-based distribution system. It is formulated as an integer linear programming (ILP) solver with the aims of minimizing transportation cost, delivery time, and flight risks across the network. Moreover, we define a location-routing problem, meaning that in a distribution system of RPASs, in addition to routing, DCs have been located in the potential sites. In this way, not only can the location of each level of DCs impact the allocation of the number of RPASs but the shipping capacity and the cost of each transport unit can differ based on the constraint of resources in the centers [16,17]. As a result, our model can analyze the maximum effective factors that are closer to the real state of distribution systems. The following conditions are defined for the model which indicates the innovation of this study.

In a real situation, it is possible to make the delivery demand at the delivery point, meaning part of the demand would be returned after the delivery. Therefore, when calculating transport costs, the customer's demand is calculated simultaneously at the time of delivery and pick-up at the demand point. At this point, the customers' demand has been met, but after the completion of delivery, RPASs return the pick-up demand to the DCs. Demand may be returned for a variety of reasons including estimated errors or incompatibility [18]. As a result, in the return route, the drones carry cargo and at the end of each graph, the demand will no longer have a decreasing trend. Therefore, it may be more or less than the demand requested from the origin in the destination node. Both pick-up and delivery demand for each route have been determined by demand points that can be changed per trip.

Assuming that many of the transported items are imperishable and there is no time limit in delivering the product would distance the model from a real situation in a distribution network, making the obtained results unreliable and incomprehensive [19]. Hence, time window management has been used as follows. Each time window determines when each delivery must take place and the model would be fined outside that timespan, be it later or sooner than the due time. This framework is implemented in the form of soft and hard windows. Combining the two mentioned modes in the routing of drones is known as the pick-up and delivery problem with time windows and demand-RPAS (PDTD-RPAS) [20]. In the RPA-based distribution network, these two aspects are rarely investigated at the same time.

Compared to land distribution systems, the distribution network of RPAs is limited to the number of RPAs and the transport capacity as their used batteries limit flight duration and change with each delivery time [21]. Therefore, enhancing their performance and assessing relevant variables in the model would increase its flexibility. In the proposed model, the possibility of charging the batteries of RPAs at some DCs has been taken into account and the estimated time has been obtained by calculating the time of charging batteries.

Factors such as uncertain weather conditions, various air traffic management errors, losing the GPS in RPASs, or security attacks [22] all cause discernible delays in delivering products or even cancel the service, which cannot be predicted in a certain situation and it is impossible to define a rigorous decision-making framework based on it [23]. For this reason, there may be different scenarios that must get as close as possible to the most certain mode before the service is complete. Therefore, in our study as the second objective, robust optimization has been applied according to the different probable traffic scenarios.

Aside from the numerous benefits associated with RPA distribution systems as an IoT setting, they are always at the highest level of vulnerability compared to other transport vehicles. This is due to the lack of sufficient and necessary instructions and security standards for RPA operations, which limits their use at the intercity level. Based on the Federal Aviation Administration (FAA), there have been over 4889 accidents of varying levels of severity caused by drones spanning 2014 to 2017 [22]. Thus, the primary need of a distribution network is to provide security against possible greater damages, which requires the identification of probable risks in the distribution. In this study, the imposed risks of selected trajectories were estimated by the Specific Operations Risk Assessment (SORA) standard, which was developed by the European Aviation Safety Agency (EASA).

Finally, since multi-objective RPAS-based location-routing problems fall into NP-Hard problems, to achieve the optimal and accurate solutions, the NSGA-II algorithm was developed. Ultimately, issued results are compared with the GAMS method in a small-scale problem to examine the model performance.

In general, the contributions of the model can be summarized as below:

- the RPAS-based distribution network of a supply chain was implemented at three echelons: facility locations, DCs, and demand points, while in other studies, path planning was not examined in more than two echelons.
- Optimization was carried out aiming to reduce three significant factors simultaneously in the model: cost, delivery time, and imposed risk. They were modeled to be minimized as the first, second, and third objective functions, respectively.
- Contrary to previous studies, constraints related to the demand, delivery time, and battery usage variables were considered simultaneously to make the model close to the real state of a distribution system.
- In the second part of the objective function in the proposed model based on different traffic scenarios, the data on the time of delivery were considered uncertain, which aims at finding answers close to optimized. Among the matters proposed to regulate uncertain data, we deployed Malloy's robust optimization model.
- In this study, the identified risks in each graph were developed in the form of a model and minimized as the third objective. For the first time, the risk assessment approach was conducted based on the SORA standard.
- In the level of distribution DCs, they were located along with RPAS routing planning.
- A novel NSGA-II algorithm was justified specifically for the introduced model.

The following parts of this study are structured as below:

Section 2 reviews previous related studies that were oriented RPA networked models with the mentioned features. Section 3 completely explains how the model is formulated and describes its components. Section 4 is organized to present solutions according to the different aspects of the model through the NSGA-II algorithm. Section 5 shows the given numerical results. Section 6 explores the results, including an analysis of the validity of the model and solutions, and ultimately, Section 7 concludes and summarizes the whole structure of the research.

2. Literature Review

The novel industry of RPA-based distribution networks is increasingly evolving. Therefore, numerous researchers in industrial or agricultural fields have attempted to propose reliable and flexible distribution models based on the characteristics and framework of RPAs.

Concerning the aspect analyzed in the previous models, Section 2.1 discusses routing problems or combined location-routing problems based on RPAs in terms of the type of variables and proposes solutions to them. Section 2.2 explores problems with certain and uncertain data as simultaneous modeling including modeling methods and their results. Section 2.3 outlines frameworks developed by companies and researchers to identify and assess the flight risks of RPAs.

2.1. Drone Routing Problem Considering Time, Demand, and Battery Constraints

In recent years, numerous studies have been conducted in this field, which has played an effective role in developing routing and location problems of distribution centers (DCs). A few of them introduce a novel routing model that proposes drone–truck combined operations [2,20,24–33]. In some, batteries can be changed at stations; in others, time windows have been used to manage the delivery time of the product, or the demand has been considered as simultaneous pick-up and delivery. For instance, based on the modeling approach, Kou et al. proposed a routing model with delivery time constraints [34]. To solve the model, the variable neighborhood search (VNS) algorithm was developed. Choi, Kitjacharoenchai, and Ribeiro et al. proposed a model based on the battery constraints of RPAs at storage room and retailer levels, which was solved using the Large Neighborhood Search (LNS) and CPLEX [21,33,35]. Khoufi et al. calculated the simultaneous pick-up and delivery demand. Time window constraints were also added and NSGA-II was used to solve the model [20]. In another study, Guerriero et al. proposed an RPA-based routing problem with multiple objectives such as reducing the distance traveled, increasing customer satisfaction, and reducing the number of used RPAs, and the Pareto Front was obtained [15]. Doole et al. used an approach derived from the traveling salesman location-routing problem to determine the shortest route the drone must travel. They applied the ant algorithm to identify the best route and select an optimal location for DCs [16].

In urban areas, due to the extensive areas for applying RPAs, numerous routing models have been developed as well; for example, Lin et al. proposed a path-planning model for RPAs considering battery consumption constraints. They introduced a two-stage control network approach which was examined by solving a numerical sample based on a virtual city [36]. Gunawardena et al. proposed a locating model for a contaminant source by RPAs. The model was implemented in a complex urban environment using particle swarm optimization (PSO). [37] Li et al. designed a routing model of logistics UAV terminal distribution in urban areas which was solved by the improved cellular automata (CA) [36].

2.2. Robust Optimization in RPA Delivery Model

Uncertain conditions could reduce the model's prediction accuracy in any aspect of location-routing problems; therefore, in previous studies, a variable, as uncertainty, Lynskey et al, was investigated along with other certain variables to analyze the direct effect of uncertainties and to propose an accurate and real model [38]. Faiz et al. designed an RPA distribution network for immediate rescue in the event of a crisis, where the demand was assumed as probable at two levels of a supply chain [39]. Lynskey et al. developed a routing model by considering atmospheric fluctuations and their impact on causing delays in the delivery time of a distribution network [38]. Cheng and Shahzaad et al. proposed an optimization approach to find an optimal flight framework with the assumption of uncertainty during the time the batteries work. In this model, the fluctuations of atmospheric temperature on the performance of the batteries were investigated [29,40]. Di Puglia Pugliese and Kim et al. introduced a robust optimization for a delivery network with uncertainty in battery consumption [41,42]. Corbetta et al. defined uncertain conditions in a state where there are probable errors during the flight, errors that differ due to types of RPAs in size and type of driving force systems and their distinctive performance during the flight [43]. S. Sawadsitang et al. developed a tri-level multi-objective model for an RPA-based distribution network that attempts to examine optimization with the probability of RPAs being endangered or unable to take off [44]. In another paper by Chauhan et al., a probable RPA-based location-routing model was introduced. The purpose behind optimization is to locate suppliers in a situation where the allocation of RPAs is never determined based on the probable usage of batteries in RPAs [16]. Ilić et al. indicated in their studies the role of RPAs in dispatching systems in smart cities. They proposed a (SWOT-FAHP) approach to improve their model [45].

2.3. Risk Assessment Model for RPA Delivery Model

The growing applications of RPAs in urban environments increase their chances of falling and hitting residents or other vehicles. Therefore, designing a risk assessment model could prevent many of those occurrences and increase the security and performance of RPAs in a distribution network. The efforts made in this regard can be assessed qualitatively and quantitatively. For instance, in their studies, Hu, Bertrand, Aminbakhsh, and Allouch et al. used both qualitative methods such as AHP and quantitative methods such as a model presentation [12,22,46,47]. Risk identification in some of them was based on international standards such as Allouch et al. [22]. Very few of them, such as Aminbakhsh et al., used the SORA standard; they identified probable dangers in different airspaces within the city with high buildings [47]. Allouch and Hu et al., by proposing a third-party risk index, showed that RPAs are at a lower risk at a height of below 30 m compared to the rest [15,22]. Janik et al. developed a risk assessment model based on SORA standard [15]. Among the methods used to assess the risk, the assessment basis in quantitative methods was based on known standards in a few cases. Most cases, however, were conducted based on professional opinions and what has been mentioned in previous studies. For instance, Shao et al. attempted to identify and estimate probable risks in a distribution network and UAS logistics by proposing UAS Traffic Management (UTM) in his paper. This assessment is qualitative and was carried out based on the SORA standard [48]. Denney et al. analyzed the SORA, whose main aim was to complete the current guidelines through a disciplined and mathematical approach for risk assessment, especially when applied to operational concepts with a greater risk that requires more accuracy in assessing and ensuring security [49]. In a paper, Capitán et al. assessed the risk of an operation for aerial shooting using the SORA method. The purpose behind using the SORA was to receive a permit for UAS flights; this paper explores all the stages of the SORA, evaluates the operational risks, and discusses corrective actions to reduce the risks in the system [50].

Analyzing the papers mentioned showed that, in most previous studies, optimization in the dimensions mentioned in certain and uncertain conditions was separately examined. However, proposing a multiple objectives model that could simultaneously analyze all the factors and can better define the real condition of an RPA-based distribution network and the obtained results are more reliable and accurate. Therefore, in addition to the development of common objectives in a distribution network such as a reduction in transport costs and delivery time, this paper introduces a robust optimization model by defining various traffic scenarios. Moreover, to increase the accuracy and efficiency of the proposed model among the risk assessment models based on international standards, in the form of the third objective, probable risks based on the SORA standard were identified. Further, the Analytic Hierarchy Process was used to allocate their proper weights and calculate the extent of their influence on transport conditions on selected routes. To make the conditions more similar to the real distribution network of RPAs, this study attempted to take into account the constraints of recharging a used battery, soft and hard time windows, and the simultaneous pick-up and delivery demand in the model. Afterward, to achieve non-dominated answers within a reasonable time, the NSGA-II algorithm was developed according to the features of the model. Further, for the accuracy test for the model, the obtained results were compared carefully using GAMS.

3. Methodology

Reviewing the most recent studies showed that location-routing optimization by RPASs has been modeled from different aspects. This study introduces a new multi-objective model integrating location-routing problem issues as a joint location-routing problem (MLRP). This model considers delivery and pick-up demands simultaneously and a time window to increase customer satisfaction. In addition, this research considers different factors affecting the stability of routes to select the best route with the lowest level of overall risk for the shipment of parcels. We try to cover all characteristics which need to be assessed in this model. It is assumed that in a three-echelon supply chain of a delivery pick up dispatching system, a set of k remotely piloted aircraft (RPA) provides services at first, for demand points at the lowest level having a set of P locations; second, a set of F facility locations at the highest level with a set of D distributors; and finally, for the level of distributors with a set of candidate locations D for construction. Locating at the second echelon occurred simultaneously as the best route is optimized in the whole process of the supply chain. The problem is modeled in the form of a multi-objective mixed-integer linear programming (MILP) model as presented below.

3.1. Objective Function

3.1.1. The Function of Cost

In our delivery network, cost includes transportation, construction of DCs, delayed delivery penalty, and preparing cost. In detail, RPASs deliver parcels to the demand points by a heterogeneous transport fleet. They have different velocities, capacities, battery consumption, and purchase costs. Therefore, to optimize the operation cost, each part of cost objective function is formulated based on its components. In our model, start points are the facility locations where the service is produced and is ready to dispatch, DCs must be allocated to a facility location. In the meanwhile, they are constructed in the potential areas. Hence, in addition to shipping costs, battery consumption and fixed costs for RPASs, the cost of building DCs, and providing services are also added to the problem. Moreover, two types of time constraints are defined for providing services to demand points. The first constraint is the hard time window, meaning that providing service to demand point i should not be earlier than b_i and the time later than α_i. The second constraint is the soft time constraint; according to it, in the period $[Es_i, Ls_i]$, service for demand point i is performed earlier than time Es_i and later than the time Ls_i. At this point, the system will be penalized, and the deviation is allowed as long as the hard time window is not violated. In this situation, service will not be provided at that time. Therefore, the cost of time windows penalties is added to the model accordingly. There are two types of demands at the demand points: the delivery demand based on which the goods are loaded from the DCs and delivered to the demand point and the pickup demand based on which the goods/services are picked up from the demand point and returned to the DCs. In this way, shipping cost may consist of pick-up demand on the way back to the DCs.

DCs are divided into two types D_1 and D_2. D_1 are those where drones can recharge at their location, and D_2 are those where drones cannot recharge at their location. Hence, D_2 will not have recharging cost at their centers.

3.1.2. The Function of Time

The time optimization is accomplished by the second objective (Z_2). As it was mentioned before, RPA velocity has different modes according to different routing scenarios while they are distinctive by the level of air traffic conditions. In a way, there is a set of U scenarios adjusted with possible routes which end in the set of j nodes. The number of scenarios is determined by experts who investigate the traffic conditions based on the following factors in the possible routes from nodes i to j.

Air traffic was happening in the RPA delivery system due to factors including:

Air parcels: The revocation or postponement was caused by situations in the control of an airline (for example, conservation or capacity issues, uploading/unloading, loading, and so on).

Severe climate: In the carrier's assessment, remarkable climatic conditions (real or predicted) cause a flight to be delayed or canceled, such as a tornado, snowstorm, or windstorm.

The National Aviation System (NAS): Postponements and revocations are provided by NAS because of various factors such as weather circumstances that are not extreme, airport procedures, high traffic volume, and air transportation management.

RPAs that are arriving tardily: A prior flight having a similar RPA had a delay in arriving, leading the current flight to depart delayed.

Safety: Postponements or revocations induced by the re-loading of RPAS as a consequence of a safety defect or unusable screening tools.

Due to the uncertainty condition of scenarios, robust optimization is the appropriate method to estimate the solutions exactly. This optimization is done while unexpected conditions are considered and controlled. We used the Mulvey model [51] as the general form of robust optimization.

3.1.3. The Function of Risk

To improve the navigation program's security and safety, the third goal proposed in this research is to minimize the overall potential risk along the flight paths. We require the capability to sort these into certain groups because several risks may be considered by the RPA dispatching system. After that, to generate relevant risk-evaluation indexes established by Erkut et al. [52], for each path, the risk index was calculated as $\sum_{(i,j)\in A} \check{p}_{ij} l_i^k$ where $\check{p}_{ij}$ and l_i^k are likelihoods for an event occurring and its repercussions, respectively. The number of valuables transported by the RPASs, weighted by the experts and historical data can be specified as l_i^k.

The significance of each component is determined by the decision makers' perspectives; however, it should be remembered that each of the risk factors stated has a distinct level of significance which is examined in each scenario in the classification of the SORA standard. Then, the linguistic variables of experts are classified in proportionate range of the adopted degrees of the assessment scale which gives $\check{p}_{ij}$. Table 1 shows the likelihood of events expressed by the frequency of their occurrence.

Table 1. Likelihood of events expressed by the frequency of its occurrence.

Rating Category	Description	Value
Certain	Expected to occur regularly under normal circumstances	10
Very likely	Expected to occur at some time	7.5
Possible	May occur at some time	5
Unlikely	Not likely to occur in normal circumstances	2.5
Rare	Could happen but probably never will	0

In the next step, to achieve l_i^k, the AHP method is applied. Accordingly, the risk of route (S_{ij}^k) is calculated based on the instructions stated as follows.

The AHP technique is used to convert these factures to a unique facture. As a result, the path risk (S_{ij}^k) is determined using the following commands:

1. Identifying and weighing efficacious risk indicators for the path (assessed by the SORA approach).
2. Employing average to specify the weights of each facture.
3. Calculating the risk of each route by applying the weights (l_i^k) assigned to the route risk variables through the equation $\sum_{(i,j)\in A} \breve{p}_{ij} l_i^k$.
4. Designing a risk matrix for the pathways from node i to node j.
5. The third goal's function is to choose the route with the minimum risk via our proposed model.

The factors must be defined before the optimization of the model, so they are calculated according to the related various features. AHP is a multi-criterion decision-making (MCDM) method for ranking several alternatives with respect to their various criteria. The AHP is applicable when the weight of proposed criteria is unknown. According to the AHP methodology, each possible route can be ranked by the risks measured in weights. They are estimated by individual experts' experiences and recorded historical data.

By taking advantage of the proposed model, the risk value can be considerably reduced with only a slight increase in the classical objective function value.

At present, risk analysis is necessary to carry out operations that go beyond the standard European scenarios. It focuses on assigning two classes of risk to a RPAS-operation, a ground risk class (GRC) and air risk class (ARC). In fact, the risk model includes risks affecting both the ground and the air.

- Ground risk elements

The ground risk class (GRC) is provided using JARUS' SORA approach by applying risk ratings generated by RPAS classifications of activities to specify the level of ground risk. The ground risk level is specified by (1) the maximum RPAS attributes such as a wingspan of 1, 3.8 m or greater, (2) their relating normal kinetic energy of 700 J, 34 kJ, 1084 kJ, or larger, and (3) operational circumstances such as VLOS, BVLOS, as well as population region, their innate RPAS ground risk levels ranging from minimum to maximum. Each different condition of class influences the severity of ground risk. The intensity of ground danger varies depending on the level. It is evident that the kinetic energy of the RPAS imposes significant damage to the people or objects on the ground.

- Air risk elements

SORA takes a more comprehensive approach to air risk management, allowing for better flexibility. This shows how reduction may be applied strategically and tactically. Flexibility is concerned with a meaningful collection of traffic density regulations with an ongoing execution function of noticing, deciding, and preventing.

The SORA utilizes three air risk categories (ARC), which ARC-b, c, and d processes require appropriate equipment stability and confidence. ARC is a descriptive rating for which an RPA might interact with manned aircraft in the National Airspace System (NAS). It is a preliminary assumption for cumulative collision risk in the airspace, before applying any reduction [53].

3.1.4. Mathematical Model

Based on the above definitions, the model can be described as follows: variables of the model have been described in Appendix A at the end of this study.

$$\begin{aligned} Z_1 = min \sum_{k\in K}\sum_{d\in v_d}\sum_{j\in v}\sum_{i\in v} X_{ijkd}\cdot FC_k\cdot dx_{ij}\cdot C + W_2\cdot \sum_{i\in p} E_i + W_3\cdot \sum_{i\in p} L_i \\ + \sum_{d\in D}\sum_{k\in K} Z_d\cdot fix_d \\ + \sum_{d\in D}\sum_{k\in K}\sum_{i\in p} X_{dikd}\cdot fix'_k + \sum_{f\in F} Y_{df}\cdot de_d\cdot Cp_f \end{aligned} \tag{1}$$

An objective function Z_1 that minimizes the total operation cost for the drones transferring, cost of battery consumption along each route, the fixed cost of using the drones, the cost of constructing distributors at candidate locations, the cost of not complying with the soft time window, and the cost of preparing.

$$Z_2 = min \sum_{u\epsilon U} p_u\cdot \sum_{i\epsilon P} s_{iu} + \lambda \sum_{u\epsilon U} p_u \left(\sum_{i\in P} s_{iu} - \sum_{u\epsilon U} p_u \sum_{i\in P} s_{iu}\right)^2 \tag{2}$$

In the second objective function, the service time is minimized.

$$Z_3 = minmax \sum_{i,j\ i\in P\cup D} s_{ij}^k X_{ijkd} \tag{3}$$

The third objective function is modeled to minimize risk index; it is measured by the sum of the imposed routing risk the weight of which is multiplied in the weights of its included components (factors) for each node i to j.

Subject to:

$$\sum_{d\in D}\sum_{k\in K}\sum_{i\in P\cup D} X_{ijkd} = 1, \forall j \in P \tag{4}$$

$$\sum_{j\in P\cup D} X_{djkd} = \sum_{i\in P\cup D} X_{jdkd}, \forall d \in D, k \in K \tag{5}$$

$$\sum_{i\in D\cup P} X_{ijkd} = \sum_{i\in D\cup P} X_{jikd}, \forall d \in D, k \in K, j \in P \tag{6}$$

$$\sum_{d\in D}\sum_{i\in v} X_{dikd} \le 1, \forall k \in K \tag{7}$$

$$\sum_{i\in D, i\ne d}\sum_{j\in P} X_{ijkd} = 0, \forall d \in D, k \in K \tag{8}$$

$$\sum_{i\in P}\sum_{j\in D, j\ne d} X_{ijkd} = 0, \forall d \in D, k \in K \tag{9}$$

$$X_{iikd} = 0, \forall d \in D, k \in K, i \in D \cup P \tag{10}$$

$$S_{iu} + \frac{dx_{ij}}{V_{ku}} - M\cdot\left(1 - X_{ijkd}\right) \le S_{ju}, \forall d \in D, k \in K, i \in D\cup P, j \in P, u \in U \tag{11}$$

$$S_{iu} + \frac{dx_{ij}}{V_{ku}} + M\cdot\left(1 - X_{ijkd}\right) \ge S_{ju}, \forall d \in D, k \in K, i \in D\cup P, j \in P, u \in U \tag{12}$$

$$S_{du} = 0, \forall d \in D, u \in U \tag{13}$$

$$a_i \le S_{iu} \le b_i, \forall i \in P, u \in U \tag{14}$$

$$LO_k = \sum_{d\in D}\sum_{i\in v}\sum_{j\in P} r_j \times X_{ijkd}, \forall k \in K \tag{15}$$

$$LO_k \le Q_k, \forall k \in K \tag{16}$$

$$L_j \ge LO_k - r_j + p_j - M\cdot\left(1 - X_{djkd}\right), \forall d \in D, k \in K, j \in P \tag{17}$$

$$L_j \leq LO_k - r_j + p_j + M\cdot\left(1 - X_{djkd}\right), \forall d \in D, k \in K, j \in P \tag{18}$$

$$L_j \geq L_i - r_j + p_j - M\cdot(1 - \sum_{d\in P}\sum_{k\in K} X_{ijkd}), \forall j \in P, \forall_i \in D \tag{19}$$

$$L_j \leq L_i - r_j + p_j + M\cdot(1 - \sum_{d\in P}\sum_{k\in K} X_{ijkd}), \forall j \in P, \forall_i \in D \tag{20}$$

$$L_j\cdot(\sum_{d\in D}\sum_{i\in P\cup D} X_{ijkd}) \leq Q_k, \forall j \in P \tag{21}$$

$$E_{iu} \geq (ES_i - S_{iu}), \forall i \in P, u \in U \tag{22}$$

$$L_{iu} \geq (S_{iu} - LS_i), \forall i \in P, u \in U \tag{23}$$

$$A_i = \text{full}, \forall i \in P_1 \tag{24}$$

$$A_i \leq A_j - DX_{ji}\cdot FC_k + M\cdot\left(1 - X_{jikd}\right), \forall i \in P_2, j \in P \cup D, k \in K, d \in D \tag{25}$$

$$A_i \geq \text{AT}, \forall i \in P \tag{26}$$

$$Z_d\cdot M \geq \sum_{k\in K}\sum_{i\in P} X_{dikd}, \forall d \in D \tag{27}$$

$$M\cdot\sum_{f\in F} Y_{df} \geq Z_d, \forall d \in D \tag{28}$$

$$de_d = \sum_{k\in K}\sum_{i\in P\cup D}\sum_{j\in P} de_d \times X_{ijkd}, \forall d \in D \tag{29}$$

$$de_d = cap_d, \forall d \in D \tag{30}$$

$$\sum_{f\in F}\sum_{d\in D} Y_{df}\cdot de_d \leq \overline{cap}_f, \forall f \in F \tag{31}$$

$$FC_k \geq S_{iu} + \frac{dx_{id}}{V_{ku}} - M\cdot(1 - X_{idkd}), \forall k \in K, i \in P, d \in D, u \in U \tag{32}$$

$$\sum_{k\in K}\sum_{i\in P\cup D}\sum_{j\in P} S_i \times X_{ijkd} \leq DAY, \forall k \in K, \tag{33}$$

$$X_{ijkd}, Z_d, Y_{df} = 0 \; or \; 1 \tag{34}$$

$$L_j, S_{iu}, LO_{dk} \geq 0 \tag{35}$$

$$s_{ij}^k \leq \mu \sum_{i\epsilon P\cup D} X_{jikd}, \forall j \in P, k \in K \tag{36}$$

$$s_{ij}^k \leq \mu \sum_{i\epsilon P\cup D} X_{ijkd}, \forall j \in P, k \in K \tag{37}$$

$$s_{ij}^k = 0, \forall j \in \mathrm{D}, k \in K \tag{38}$$

Constraint (4) ensures that a RPA is allocated to one demand point and meets its demand. Constraint (5) ensures that any RPA leaving the DC finally returns to the same DC. Constraint (6) ensures that any RPA that allocated to a node to provide service to any demand point. Constraint (7) ensures that every RPA is applied in just one distributor. Constraints (8) and (9) ensure that if a RPA leaves a DC, that RPA is assigned only to that DC. Constraint (10) ensures that no additional edges stem from each node to itself. Constraints (11) and (12) examine the starting time of service for per demand point. Constraint (13) mentions that the start time of the RPA is zero. Constraint (14) ensures compliance with the hard time window limit. Constraint (15) calculates the quantity of first loading of the RPA.

Constraint (16) examines the capacity limitation of the RPA for the first loading. Constraints (17) and (18) calculate the loading weight on the RPA after leaving the initial demand point across the route. Constraints (19) and (20) calculate loading weight on the

RPA after leaving other demand points. Constraint (21) ensures that the RPA capacity limitation for loading weight on the RPA across the route. Constraints (22) and (23) calculate the soft time window deviation for demand points. Constraint (24) illustrates that after the service to demand points with charging availability, battery is full in the RPA. Constraint (25) calculates the amount of battery in the RPA after finishing service to demand points where recharging is available. Constraint (26) ensures that the RPA battery constraint is considered. Constraint (27) indicates constructed DCs. Constraint (28) ensures that each DC constructed and assigned to one facility location. Constraint (29) calculates the amount of demand for each DC. Constraint (30) determines the demand limitation of each DC. Constraint (31) examines the demand limitation of each facility location. Constraint (32) calculates the travel time for every RPA. Constraint (33) investigates the time limitation of the travel length daily. Constraint (34) demonstrates the variables zero and one. Constraint (35) demonstrates variables greater than or equal to zero. Constraint (36) ensures that the imposed risk for route i to j is lower than M denotes a large positive constant. Constraint (37) ensures that the imposed risk for route j to i is lower than M denotes a large positive constant. Constraint (38) ensures that the risk of routes ending in facility locations is zero.

3.1.5. Assumptions

- The drones make one-to-many delivery trips at the first echelon (from the facility location to the DCs) and many-to-many trips at the second echelon (from DCs to demand points and back) until the battery needs to be re-charged. It includes a minimum energy also set for emergencies.
- We do not consider one-to-many vehicle routing type trips, which are consistent with the initial applications of RPA deliveries by private companies.
- We also do not consider battery recharging during the planning period for DCs where recharging is not possible and assume that the RPA battery is recharged between planning periods, but for those where it is possible, the service time at each site includes refueling time (time to recharge the RPA's battery), if needed.
- The length of the planning period is shorter (6 h to a day or 2 days) compared with the planning period for a typical facility location problem.
- Another important assumption for the development of the mathematical model is related to the first m actions. They are dummy event locations used to represent the RPAS's initial positions. Thus, no time windows are associated with these events, but they are simply born at the scenario starting time instant and remain active for all durations of the scenario itself.
- We refer to the RPA as any aircraft capable of moving autonomously at varied and heterogeneous velocity, capacity, battery consumption, and purchasing cost.
- Each RPA can serve more than one demand point per dispatch as long as its flight range and load carrying capacity are not violated.
- RPAs can return to the same DCs along the route.
- Multiple RPAs can be dispatched simultaneously from any DCs, which allows the use of a swarm of RPAs to enhance the overall productivity of the system.
- We assume that applied RPAs have the battery capacity to cover the longest planning period, and before per dispatch, operators ensure that drones have enough battery to the end of the route.
- There are limited DCs equipped with recharging stations
- Customers are served only by RPAs.
- RPAs can be dispatched and collected several times from the same DCs.
- RPA batteries are replaced with fully charged batteries each time.
- Packages are loaded and unloaded from the RPAs once the RPAs deliver to DCs or demand points.

- After battery replacement and package loading/unloading, the RPA can be dispatched again to serve a new set of demand points. The process is repeated until all demand points in the service area have been reached.

4. Solution Representation

By combining several aspects of the location-routing problems, a multi-objective Location-Routing problem with Drones (LRPD) model was developed, which is considered an NP-Hard problem in terms of dimensions and the required time to solve it. Therefore, metaheuristic algorithms could optimize all three objectives during a reasonable time and obtain a set of efficient answers considering the constraints. In this study, the NSGA-II algorithm was developed to solve the model. Selecting the best solution among each generation of solutions is the development basis of this model. We deployed a novel approach to generate the initial population which is based on the total number of demand points and RPAs. The following sections describe the methodology of it in our developed algorithm. Moreover, for the reliability and efficiency test of the model, the problem was solved on a small scale and then assessed.

All the numerical experiments were conducted in MATLAB software and on a Laptop with Intel Core I7 Duo 3.7 GHz and 8 GB RAM.

4.1. Non-Dominated Arranging Genetic Algorithm II NSGA-II's Construction

NSGA-II is a famous algorithm established by Pareto solutions notions that were initially created by [54]. Unlike single-objective issues, multi-objective issues do not have an optimum solution. As a result of this algorithm, which is described as the non-dominated sorting genetic algorithm (NSGA-II), a collection of practical non-dominated solutions is developed. For non-dominant population rating, the method initially selects two parental solutions from which they continuously retrieve a superior child solution via an intersecting function.

To establish if a solution is dominant or non-dominant, it should initially be analogized with every other solution. A category of solutions will be discovered, none of which are dominant or non-dominant, and these solutions will also include the initial front of non-dominant fronts. Available solutions are ignored throughout the initial front and then continued using the idea of dominance to define additional fronts. Indeed, a solution x will triumph over a solution y if the following criteria are met:

- Solution x is not worse than another solution y for any of the goal's functions.
- x is strictly superior to y in at least one of the n goal's functions. This procedure will be repeated until all non-dominant solutions have been eliminated.

The following characteristics may be found in several NSGA-II algorithm elements.

4.1.1. Initial Population

The initial population is divided into three groups. There are $n + k - 1$ cells in the first segment. The starting population is produced by a line with $n + k - 1$ cells having ordinal numbers 1 to $n + k - 1$, where n is the number of demand points and k is the number of RPAs. The numbers 1 to n represent the number of demand locations, while the numbers $n + 1$ to $n + k - 1$ represent RPAs delivery to distribution facilities and in the other way, the endpoint of the path and the usage of another RPA. The sequence of services to the demand points is shown by the placement of the numbers in the columns. RPA k is represented by the number $n + k$ which represents the demand points that may be handled by that RPA, correspondingly. If the demand point number is not before the RPA number, it means that the RPA has not been used and that none of the RPAs have been allocated to it. After the final RPA number, all demand points are allocated to the last RPA, correspondingly. RPAs are allocated to RPAs in this segment. The second portion has $k + d - 1$ cells, where k is the number of RPAs and d is the number of possible placements for DCs. This segment, like the previous one, is devoted to distribution facilities. The final part is made up of $d + f - 1$ cells, where d represents the number of DCs and f represents the number of sites.

In this segment, the employed DCs are assigned to the sites in the same manner as in the previous two segments.

To illustrate further, an example of the original population is provided. Figures 1–4 show an example with eight demand points, three RPAs, and three distributor candidate sites. In the first segment, the scores 1 through 8 represent demand points, while 9 and 10 represent the first and second distributors. Demand points 4, 6, and 8 are supplied by the first RPA, demand points 1 and 3 are handled by the second RPA, and demand points 7, 2, and 5 are supplied by the third RPA, as seen in Figure 1. In the following segment, the numerals 1 through 3 represent the number of RPAs, while the numbers 4 and 5 represent the first and second distributors. According to the proposed approach, the first and second RPAs are assigned to distributor 1, and the third RPA is assigned to distributor 2. Distributor 3 has not been built to this level yet. In the third segment, the numbers 1 through 3 represent the number of distributors, while the number 4 represents the initial facility sites. According to the solution in Table 2, distributor number 1 is assigned to the second facility site, whereas distributor number 2 is assigned to the second facility site.

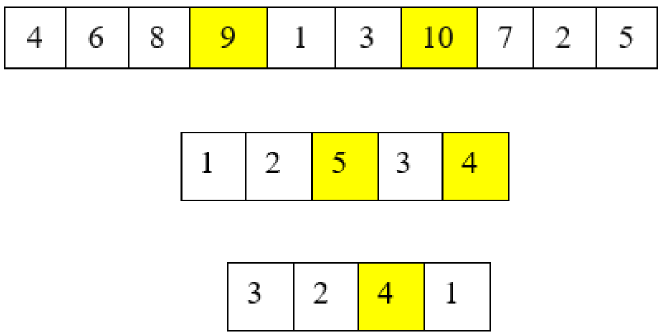

Figure 1. Example of the solution matrix.

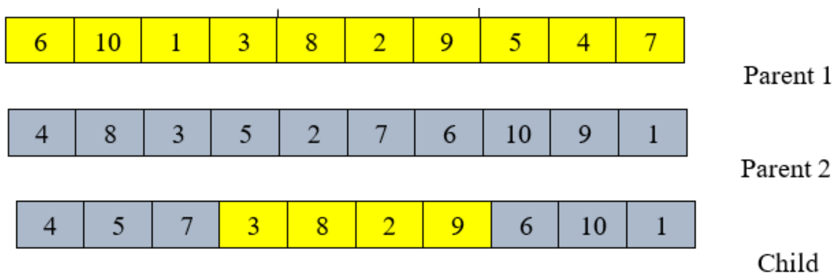

Figure 2. Crossover operator for each part.

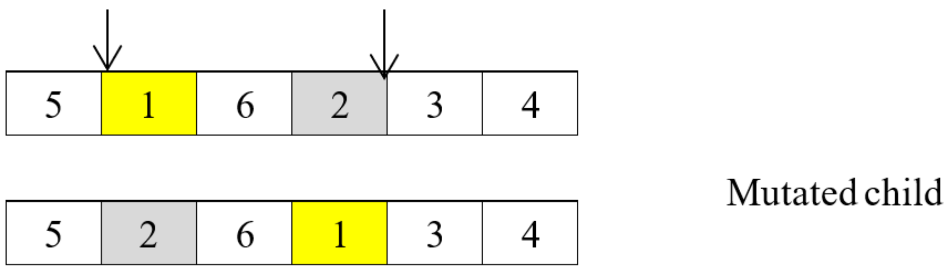

Figure 3. Mutation operation for each parent.

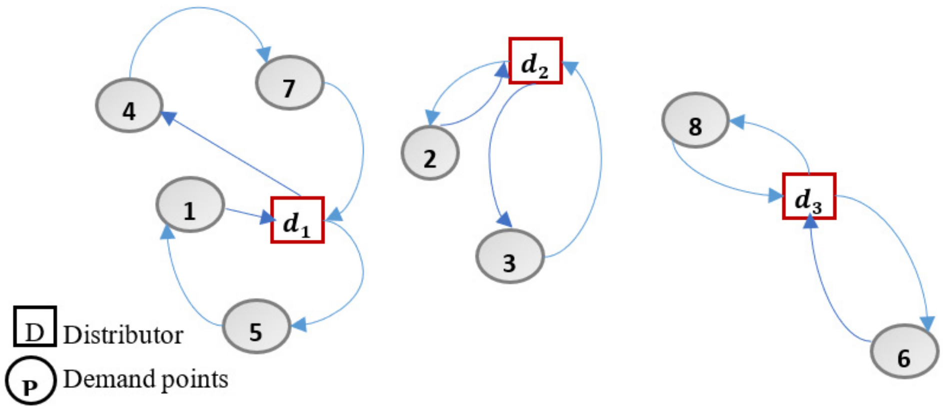

Figure 4. Problem solving by GAMS.

Table 2. Solution of example.

Demand Points	Distributor	Number of RPA	Route
2	1	1	4-6-8
2	1	2	1-3
1	2	3	7-2-5

4.1.2. Parents Selection

When the adaptability of the goal functions among each chromosome is determined and the population is sorted based on the requirements of domination, new parents form a new population. In other words, superior individuals have a better probability of marrying and passing on their characteristics to another generation. The tournament selection method is employed to pick each parent. In this procedure, two individuals are chosen randomly, and the best of these are chosen to become parents. A similar procedure is followed to choose the next parent.

4.1.3. The Crossover Operator to Produce New Children

Following the selection of two parents using the tournament technique, the two-point intersecting method is used to generate additional offspring, with two intersecting points chosen randomly for each section of the initial two-by-two solution. The genes from the first parent among these two points are given straight to the first kid, whereas the leftover genes in the second parent are transcribed to the first child.

If the born children fulfill the capacity and time limitations, they enter the new generation; otherwise, two parents are chosen randomly for the intersecting. This procedure is repeated until the new offspring outperforms its parents in terms of adequate function. In the time frame limitation, for instance, if the kid is born inside the set window of time, it will be counted as a new generation; in this situation, the carrying time will be modified.

4.1.4. Mutation Operator

When the intersecting operator is accomplished, the mutation operator is applied to the following step. In this algorithm, both operators are hunting for fresh space. The neighborhood hunt is done using this operator to increase the variety of a newly produced population, and the search space is expanded to attain the complete optimal. Each offspring throughout this operator can change randomly to generate a random number. If this score is smaller than the mutation rate, the offspring will be modified by the mutation operator in a manner that the first two genes are picked randomly, then the numbers between them are switched for a genetic mutation.

Following the formation of a novel generation of Pareto solutions, grouping is conducted by utilizing the non-dominance value and crowding distance. If two populations come from separate fronts, the solution with the lowest front number is chosen; if they come from a certain front, the solution with the maximum crowding distance is chosen to establish a mating pool.

Eventually, the grouping technique is used to create a population of precise size, NPOP (Number of Population). By repeating the preceding procedures in succession, the new population is employed to develop the next new offspring. This procedure is continued until the halting condition is satisfied. A set number of iterations is used as the terminating factor.

5. Computational Result

To validate and prove the accuracy of the model, a problem with 8 demand centers, 4 candid locations for DCs, 4 facilities, 3 RPA models, and 5 probable scenarios for air traffic was randomly created on GAMS. Thus, conformance to the constraints and the values of the three objective functions were evaluated. Figure 4 illustrates the schematics of the results obtained through GAMS. As apparent, the location of the fourth candidate was eliminated while all the RPAs were allocated to DCs.

In the next step, to ensure compliance with delivery time constraints and transport capacity in the model, Figures 5–8 are proposed to demonstrate the constraints of hard and soft time windows and transport capacity on each route based on the characteristics of the examined RPA, respectively. Figure 7 indicates the initial loading constraint and Figure 8 present the weight constraints of RPA transport on permitted flight trajectories. In Figure 7, number 1 indicates distributor 1 from route 1, number 2 indicates distributor 1 from route 2, number 3 indicates distributor 2 from route 1, number 4 indicates distributor 2 from route 2, number 5 indicates distributor 3 from route 1, number 7 indicates distributor 4 from route 1, and number 8 indicates distributor 4 from route 2.

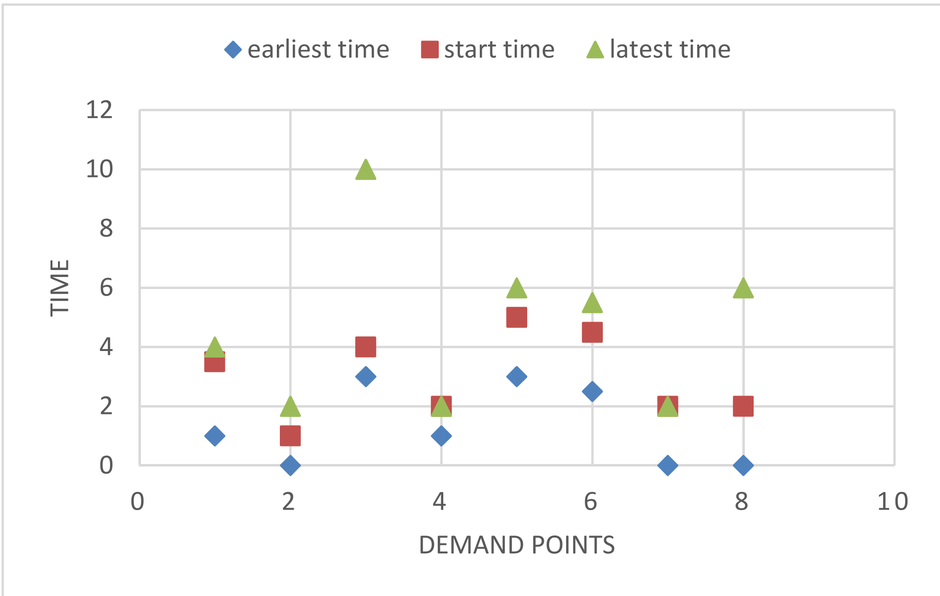

Figure 5. Compliance check for soft time windows.

5.1. Input Data for NSGA-II Parameters

To assess the model, the developed NSGA-II algorithm was solved through a small-scale problem and the results are compared using GAMS. In this sense, we elaborate sequential solution of the model through the following sections. In this model, the parameters of the algorithm were determined using the Taguchi method as depicted in Table 3.

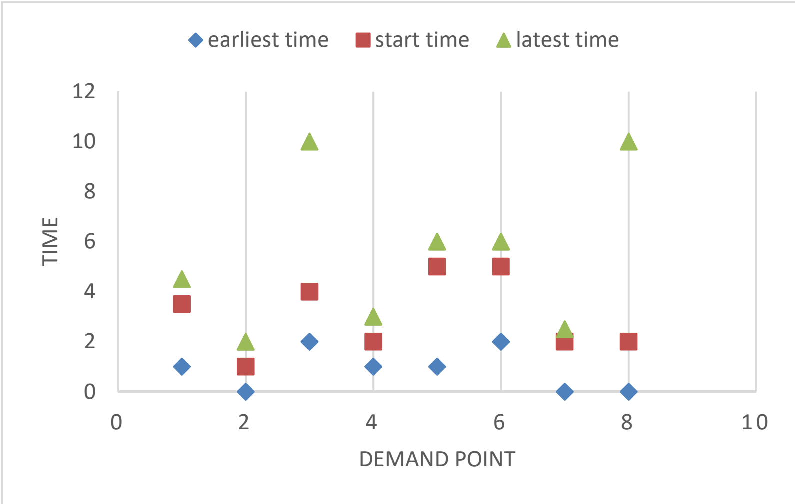

Figure 6. Compliance check for hard time windows.

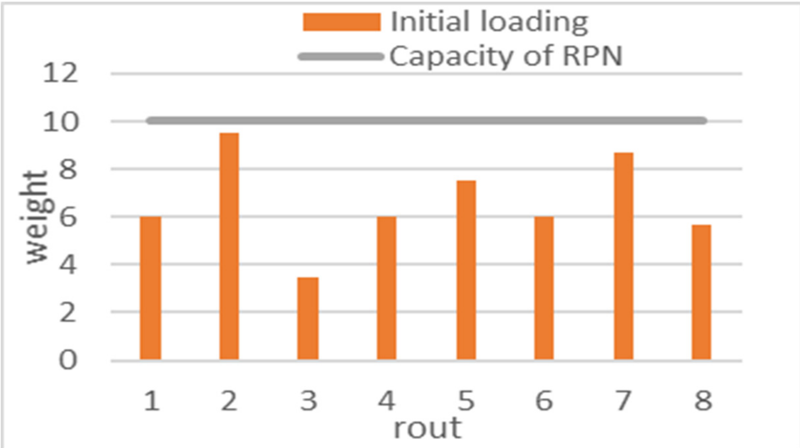

Figure 7. Compliance check for initial loading constraint.

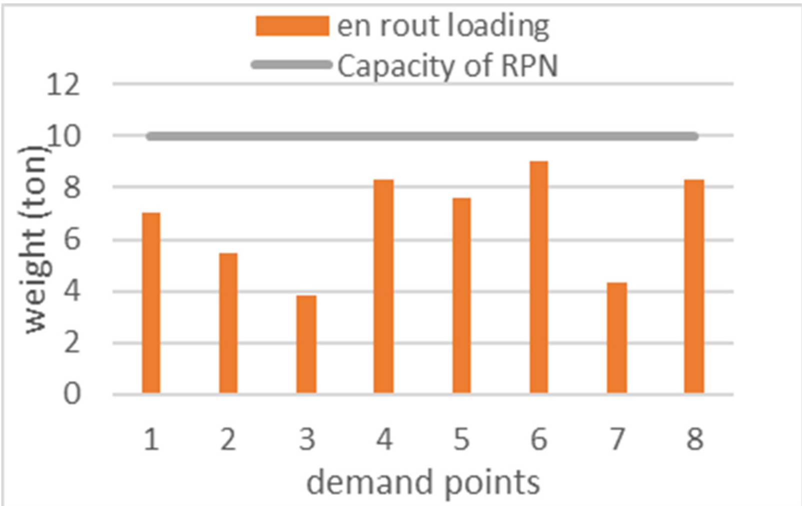

Figure 8. Compliance check for end route loading constraint.

Table 3. Parameters for NSGA-II.

NSGA-II	Value
npop	50
maxit	400
P_C	0.4
P_m	0.7

5.2. Input Data for Risk Model Parameters

This section calculates the input risk indices for each route. According to the mentioned stages, in Section 3.1.3, determining factors in the risk of each route are categorized as air or ground risks based on the SORA standard, which covers all the stages of RPA operations from the pre-flight stages such as take-off to in-flight failures in RPAs such as the excessive use of batteries in harsh weather conditions to post-landing. In this location-routing model with RPAs, the distribution network was considered in the urban environment, which further increased the chances of an accident for RPAs in a flight at a low height. In the SORA standard, the investigated risk level varies depending on the fly zone, and factors such as the region's population and the type of applied RPA play a role.

SORA categorizes operational safety objectives (OSO) into the following categories:

- The RPA has a technical issue (OSO # 1-OSO # 10);
- External systems that support RPA functioning are deteriorating. (OSO # 11-OSO # 13);
- Errors made by individuals (OSO # 14-OSO # 20);
- Unpleasant performing conditions (OSO # 21-OSO # 24) [48].

According to the SORA categorization, we believe RPA will be conducted in VLOS (Visual Line of Sight) on infrastructure and individuals. We suppose that a Hexa-rotor RPA is deployed to deliver a delivery weighing 12 kg. The RPA flies at 5–8 m/s and travels at 35–50 m AGL, quicker than 40 min. This represents the current state-of-the-art and a typical RPA platform being used in many ongoing delivery tests and trials.

The first step in determining the hazard of an operation is to calculate the value of the kinetic energy that the RPA may have. The hazard analysis data are as below, calculated with the following Formula (39) and the manufacturer's data:

$$E_k = \frac{mv^2}{2} \tag{39}$$

E_k = kinetic energy (J), m-mass (kg), v-velocity $\left[\frac{m}{s}\right]$ [55].

a. Selected RPA: Arm pitch 83 cm hexa-rotor, Maximum Take-off Weight (MTOW) m = 12 kg, cruise speed v = 8 m/s.
b. Population: n/SS = high populated (10,000 n/m^2 or 3853 n/km^2).
c. Arm pitch 0.83 $\times$ 0.83 m from a hexa-rotor.
d. Kinetic energy of RPA (KE): 384 Joules, from a hexa-rotor.
e. MTOW (m): 12 kg.
f. Velocity (v): 8 m/s (maximum operating speed of hexa-rotor H83)

The hazard level is analyzed by the likelihood of probable occurrences between selected routes considering the main elements of ground risk and air risk of the SORA standard, based on the given features of the used RPA. It should be mentioned that the innate ground risk (GRC) may be calculated using this data. The flight during the real incident might have to be classified as VLOS over a populated area. This flight type has a GRC of 5 on the present 10-point scale, as given in Table 4.

Table 4. Intrinsic ground risk (GRC) determination [48].

Max UAS Characteristics	1 m/Approx. 3 ft	3 m/Approx. 10 ft	8 m/Approx. 25 ft	>8 m/Approx. 25 ft
Typical kinetic energy Expected	<700 J (approx. 529 Ft Lb)	<34 KJ (approx. 25,000 Ft Lb)	<1084 KJ (approx. 800,000 Ft Lb)	1084 KJ (approx. 800,000 Ft Lb)
Operational scenarios				
VLOS/BVLOS over controlled ground area	1	2	3	4
VLOS in sparsely populated environment	2	3	4	5
BVLOS in sparsely Populated	3	4	5	6
VLOS in populated Environment	4	5	6	8
BVLOS in populated Environment	5	6	8	10
VLOS over gathering of people	7			
BVLOS over gathering of people	8			

5.3. AHP Ranking Method

As a result of the circumstances, each of them provides feedback at various phases of the service AHP, which is a Multi Criteria Decision Making (MCDM) approach that is used to handle a variety of analytical hierarchical issues efficiently [56,57]. AHP is employed to compare risk variables related with human error and incident generates in the marine transportation industry. Relying on a pairwise analogy matrix of criteria and options, AHP assesses both quantitative and qualitative factors. The AHP idea is for analytical decision-making, allowing the decision-maker to select the best choice from a collection of options associated with a set of criteria.

The capacity of AHP to verify and decrease the variance of expert opinions is its major benefit. At the same time, eliminating bias in decision making, assigning properties to each criterion, merging qualitative and quantitative assessments, and powerful systematization are all aspects of this procedure.

In this research, AHP is utilized to generate a matrix of weighted risks of $S_n = \{1, \ldots, n\}$, where n is the number of possible nodes between points i and j in each level of supply chain management. At this moment, we execute the following phases of the process:

1. Create an enforced routing risk matrix, $S = \left\{S_{ije}\right\}_{m \times n}$, with $m = n$ representing the number of risk criteria. The criteria are based on the SORA approach and contain elements that influence the occurrence of events that cause an incident.

In reality, the issue choice (probability of occurrence in our research) is frequently separated into a hierarchy of sub-problems (adverse event causes), each of which may be evaluated separately.

2. Experts provide a numerical scale to each pairing of n criteria (S_i, S_j) at the first level of hierarchy.

According to experts in our research, it is vital to include the personnel operating the RPA in detecting difficulties early in the history of the service. They assist in the delivery of the service and have direct interaction with the customer.

Furthermore, it is suggested in the proposed strategy to incorporate staff of the organizations offering the service at the client's location in the risk inspection process. Their expertise and experience are crucial in determining the reasons for recognized unfavorable occurrences and analyzing the repercussions of their occurrence [58]. As a consequence, since their perspective is very analytical, staff of service organizations should actively engage in defining the grounds of the deployment.

Numerical scales are assigned by performing pairwise comparisons among the criteria in terms of their influence on an element at a higher level in the hierarchy. The scale runs from one to nine, with both numbers indicating an important rating. Table 5 illustrates these results.

Table 5. The importance values of numerical scales.

Importance Scale	Definition of Importance Scale
1	Equally important preferred
2	Equally to moderately important preferred
3	Moderately important preferred
4	Moderately to strongly important preferred
5	Strongly important preferred
6	Strongly to very strongly important preferred
7	Very strongly important preferred
8	Very strongly to extremely important preferred
9	Extremely important preferred

The concept S_{ije} refers to expert e's personal preference for criterion S_i over S_j.

3. Once all the experts express their judgement, the geometric mean of their values are computed as follows:

$$S_{ij} = \sqrt{S_{ij1}}, \; S_{ij2}, \; S_{ij3} \tag{40}$$

The acquired S_{ij} is then placed as its input into the matrix D:

$$D = \begin{bmatrix} S_{11} & \cdots & S_{1m} \\ \vdots & \ddots & \vdots \\ S_{n1} & \cdots & S_{nm} \end{bmatrix}$$

4. At this stage, the weights of the criteria are computed by summing the columns of the normalized Matrix W, which, as said by Saati [59], is a comparison matrix with the following attributes.

$$S_{ij} > 0; \; S_{ij} = \frac{1}{S_{ji}} \; \forall_i \; where \; j = 1, 2, \ldots.., n \tag{41}$$

When the elements of Matrix W meet the requirement while also satisfying the condition, it is said to be consistent (2):

$$S_{ij} \times S_{je} = S_{ie} \; \forall_e \; where \; j = 1, 2, \ldots.., n \tag{42}$$

The arrangement of options is determined by utilizing a matrix to approximate the comparison matrix W.

$$P = \begin{bmatrix} P_{11} & \cdots & P_{1m} \\ \vdots & \ddots & \vdots \\ P_{n1} & \cdots & P_{nm} \end{bmatrix}$$

The components of matrix W are consistent assessments provided as weight ratios between criteria $S_{ij} = \frac{S_i}{S_j}$ where i, j = 1, 2, ..., n

The weights of the criteria of the order vector p are indicated by P_i.

$$P = (P_1,\ P_2, \ldots.., \ P_n)^T$$

Following arithmetic normalization, the standardized order vector looks like this

$$P^* = (P_1{}^*,\ P_2{}^*, \ldots.., \ P_n{}^*)^T$$

where

$$P^* = \frac{p_i}{\sum_{i=0}^{n} p_i}$$

Erkut et al. suggested determining the assessment matrices using the maximum eigenvalue approach, as follows [52]:

$$D{\cdot}P = \lambda_{max}{\cdot}P\ \lambda_{max} > n$$

where λ_{max} is the matrix W's maximal eigenvalue.

It is vital to highlight that the inconsistency of the comparison matrix W has to be less than 10% for a valid comparison, this is, the number of moments condition (2) is not fulfilled must be fewer than 10%.

Computation should be conducted numerous times to form a conclusion when confronted with an incompatible matrix to achieve convergence among the set of solutions into subsequent repetition of this procedure. The original data are then transformed into understandable absolute values and normalized weights using the following formula: w = (w_1, w_2, w_3, . . . , w_n):

The consistency of assessments, as said by [52], may also be examined utilizing Equation (9).

$$\text{Consistency ratio} = CR = \frac{CI}{RC} \tag{43}$$

and,

$$\text{Consistency index} = CI = \frac{\lambda_{max} - n}{n - 1} \tag{44}$$

Table 6 has the RC (random consistency index). Because all 1 × 1 or 2 × 2 comparison matrices include dependent column(s), RC is considered to be 0. It leads CR to go toward infinity, i.e., matrices with sizes 1 and 2 are often consistent.

Table 6. Random consistency (RC) index (n = size of the reciprocal matrix).

n	**1**	**2**	**3**	**4**	**5**	**6**	**7**	**8**	**9**	**10**
RC	0	0	0.58	0.9	1.12	1.24	1.32	1.41	1.45	1.49

5. In the final matrix S_{ij}, rank the criteria in decreasing order of the computed values; the inputs of S_{ij} are used as the value of s_{ij}^k in Equation (39).

According to the steps above, s_{ij}^k matrix is achieved as Table 7 with the following assumed input data: 3 distributors, 8 demand points, and 3 RPAs.

Table 7. The resulting s_{ij}^{k} matrix through the AHP method.

				RPA 1				
s_{ij}^{k}	**1**	**2**	**3**	**4**	**5**	**6**	**7**	**8**
1	167	60	28	87	176	56	234	34
2	117	39	40	83	123	34	256	47
3	123	121	22	22	147	78	278	67
				RPA 2				
1	147	78	36	90	144	43	246	46
2	123	43	57	61	187	45	215	67
3	136	134	17	15	245	81	209	89
				RPA 3				
1	193	56	28	84	148	57	296	59
2	119	68	57	62	197	43	257	54
3	142	123	19	14	223	79	211	68

6. Results and Discussion

Table 8 demonstrates the results of the objective function differentiation using GAMS and NSGA-II. The difference between the results of both methods indicates that the performance of the algorithm with a small-scale problem, less than ten, is less different from its exact method. However, an increase in the scale of the problem increases the duration of its implementation in the exact method, even though not much difference can be observed in the optimal value of objective functions in both the rigorous and metaheuristic methods.

Table 8. Comparison of the answer of NSGA-II with the exact solution in small sizes.

Number of Demand Points	**NSGA-II**				**GAMS**			
	Z_1	Z_2	Z_3	**Elapsed Time(s)**	Z_1	Z_2	Z_3	**Elapsed Time(s)**
N = 4	449,297,460	10,004	9978	56.43	449,297,478	1049	9967	78.65
N = 5	650,779,184	15,613	10,310	56.153	650,779,184	15,620	10,311	109.34
N = 6	602,471,673	11,643	12,347	60.300	602,471,513	11,640	11,981	123.56
N = 7	487,170,264	15,486	11,219	53.99	487,350,634	15,590	11,209	168.43
N = 8	669,350,742	12,305	10,267	56.040	669,350,736	12,307	10,236	172.78
N = 9	674,892,002	14,822	10,290	57.90	674,891,988	14,903	10,293	193.2
N = 10	674,066,352	12,822	11,709	53.224	674,066,367	12,945	11,734	214.93

Figure 9 illustrates a set of Pareto Front answers to all three objective functions. The dispersion of the obtained points can be observed in all the points of the objective function. The convergence process of the algorithm shows that considering the used operators, the algorithm has not fallen to the local optimum, and in the generated generations, most of the objective function space has been analyzed in the 400th iteration.

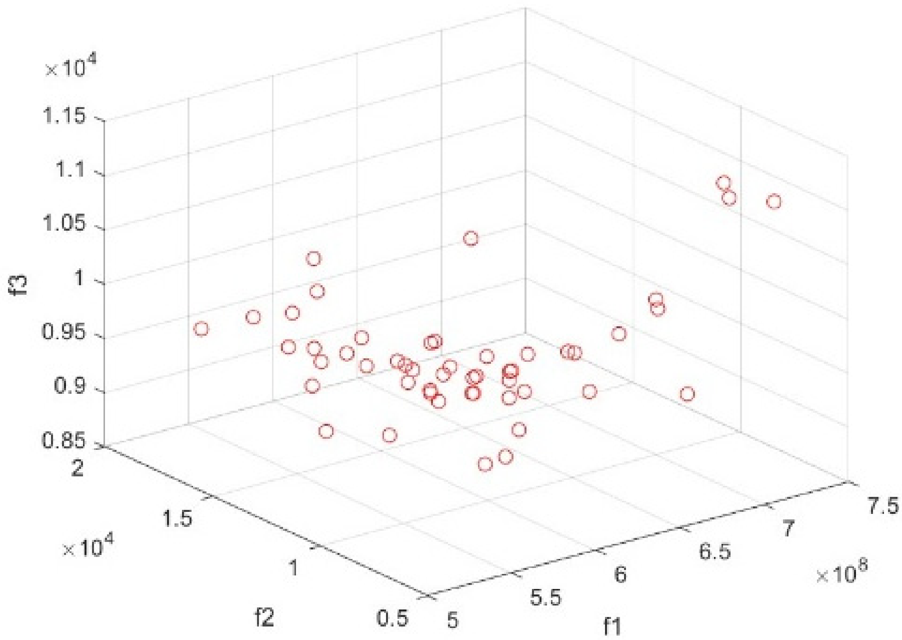

Figure 9. The Pareto Front chart of sample 8 by NSGA-II algorithm.

Figure 10 also demonstrates the convergence process of each objective function.

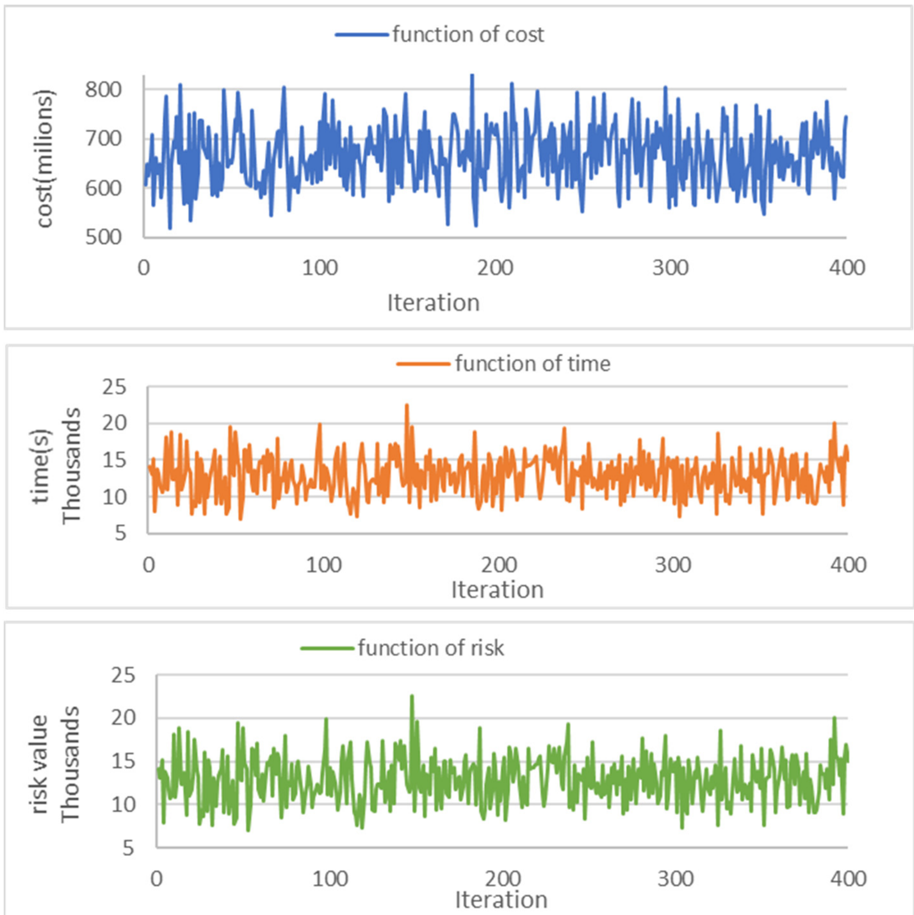

Figure 10. Schematic view of objective functions convergence by iteration.

To practically assess the model, the optimal value of the Pareto Front during each iteration is compared in Table 8. Objective functions were optimized with different scales of problem to show the accuracy of the model. Furthermore, it indicates how the proposed NSGA-II algorithm will behave when more points needs to be investigated in a location-routing model. The improvement process of objective functions shows that each objective function has drastically declined. However, it is not possible to determine a specific value for each as the most optimal specific value to define multiple objective functions, and based on their priorities in decision-making, the decision-makers prefer the optimization of one objective function over the other. For example, if the minimum transport cost and a rise in the security of distribution systems are in question, in a problem with 8 demand points, Z_1 decreases by 35.40%, Z_2 by 56.79%, and Z_3 by 28.90%. Table 9 illustrates the analysis of the sensitivity of the model based on its parameters such as time variation in different scenarios in the second objective function with 8 demand points. The lighter the air traffic, the shorter the distribution time. The selected route will also differ.

Table 9. Comparison of objective functions value in different scenarios.

Scenarios	PS	Optimal Solution	Activated Location	Z_1	Z_2	Z_3
1	0.03	1 → (1,5)_(5,4)_(4,7) 2 → (2,3) 3 → (6,8)	1,2,3	669,350,742	1.2305	10,267
2	0.04	1 → (1,5)_(5,4)_(4,7) 2 → (2,3) 3 → (6,8)				

In this table, two scenarios with the most estimated time in the nodes are determined along with the probability of their occurrence (PS). In both, the values of the first and third objective functions remain unchanged while the second objective function slightly decreases. Interestingly, the optimal routing in the second scenario, with the shortest estimated time, has remained unchanged like the first scenario, which indicates that the first robust model presented shows the most optimal legitimate solutions in any traffic mode with high accuracy. By taking into account that there is not much difference in the values of the objective function, it can be concluded that the model gives identical results if the probable scenarios are disregarded.

Additionally, in multi-objective optimization models, the defined objectives do not get minimized and optimized in one way, and a decrease in a minimization problem may lead to an increase in the other. Therefore, the optimization behavior of each of them during the implementation of the algorithm is analyzed to determine the accuracy and precision of the obtained Pareto Front. Therefore, Table 10 shows the pay-off and how, in the case of the optimization of one objective function, the rest has changed.

Table 10. Pay off table of problem.

The Objective Function	Z_1	Z_2	Z_3
Z_1	627,592,605	11,155	9311
Z_2	727,991,324	7321	9366
Z_3	820,942,970	14,059	8661

The process of the objective function values shows that a decrease in Z_1 would increase Z_2 and Z_3. Further, a decrease in Z_2 would increase Z_1 and Z_3, while a decrease in Z_3 would increase Z_2 and Z_1. As a result, the optimization process of objective functions is the opposite of each other.

Parameters Analysis

In most proposed models, a change in the defined parameters could drastically impact the obtained results. If the results remain unchanged or slightly changed despite great changes in the input parameters, the model has high efficiency and accurate performance. Therefore, Table 11 was obtained through an increase in the costs of the transport unit.

Table 11. Sensitive analysis of goals value.

Z_1 (Cost)	Z_2 (Time)	Z_3 (Risk)	Cost (fix'_k)	Activate Location	Optimal Solution for Locations
669,350,742	12,305	10,267	496	1,2,3	1 → (1,5)-(5,4)-(4,7) 2 → (2,3) 3 → (6,8)
449,989,508	18,749	10,836	478	1,2,3	1 → (1,5)-(5,4)-(4,7) 2 → (2,3) 3 → (6,8)
426,296,864	14,888	11,679	356	1,2,3,4	4 → (4,7) 2 → (2,3) 3 → (6,8) 1 → (1,5)
412,789,234	19,329	11,345	280	1,2,3	1 → (1,5)-(5,4)-(4,7) 2 → (2,3) 3 → (6,8)
367,879,215	21,354	11,236	130	1,2,3,4	4 → (4,7) 2 → (2,3) 3 → (6,8) 1 → (1,5)

As can be observed from Table 8, with a decrease in the parameter of the fixed cost of each RPA, the cost function decreases, whereas, the robust function of delivery time increases but not much change can be seen in the risk function. Although the optimal route was changed, the three candidate locations 1, 2, and 3 were chosen for the construction of DCs in any state of unit cost. This shows that in each state of cost change, the mentioned locations are efficient for the construction of DCs.

7. Conclusions

This study has proposed an RPA-based multi-objective location-routing distribution network for notional delivery RPAS incorporating air and ground risk assessments. The model is characterized by hard and soft time windows, pick-up and delivery demand, and battery consumption limitations; and through the objectives of the model, robust optimization is applied to reduce delivery time then the model is solved by the developed NSGA-II algorithm. The results reveal that although numerous factors could be effective in a distribution operation, it is possible to control flight security in each aspect of the distribution and delivery operations including cargo transport, delivery time, and used battery capacity. According to the results, the proposed model has been able to optimize all three objectives and decline by 31.9% on average. Furthermore, its slight difference with the results of the GAMS method indicates the success of the NSGA-II algorithm in solving the model. In addition, although different scenarios are determined, candidate locations (1,2,3) and the selected path have remained unchanged for both scenarios which shows the consistency and reliability of the model

Along with all the mentioned advantages of our model, this study confronted serious errors in practice which need to be considered for future research. In more detail, in optimizing the second objective function, uncertainties in air traffic conditions can be categorized as several scenarios, but it is difficult to determine which scenario is most likely to occur. Therefore, we assigned two scenarios that can be clearly near to the real state of potential routes. In addition to this, in the process of analysis of the imposed risks, as the expert's opinions are linguistic variables, it was a time-consuming approach to classify them with respect to the SORA standards categories.

Author Contributions: Conceptualization by J.L., R.C.M. and A.M., methodology by L.H. and A.M., investigation by all, writing—original draft preparation by L.H. and A.M., writing—review and editing by all and supervision R.C.M. and J.L. All authors have read and agreed to the published version of the manuscript.

Funding: This research was funded by "the Carleton University: international seed grant".

Institutional Review Board Statement: Not applicable.

Informed Consent Statement: Not applicable.

Data Availability Statement: The data presented in this study are available on request from the corresponding author.

Conflicts of Interest: The authors declare no conflict of interest.

Abbreviations

RPAS	Remotely Piloted Aircraft System
SORA	Specific Operation Risk Assessment
ICT	Information and Communications Technology
DC	Distribution Center
IOT	Internet of Things
FAA	Federal Aviation Administration
EASA	European Aviation Safety Agency
MLRP	Multi-objective Location-Routing Problem
NAS	National Aviation System
MCDM	Multi Criteria Decision Making
LRPD	Location-Routing problem with Drones
ARC	Air risk class
GRC	Ground risk class
MTOW	Maximum Take-off Weight
OSO	Operational safety objectives
NPOP	Number of Population
NSGA-II	Non-dominated sorting genetic algorithm II

Appendix A

sets

Decision Variables	
D:	A set of distributor candidate locations
F:	A set of facility locations
P:	A set of demand points
K:	A set of drones
D_1:	A set of demand points where recharging is possible
D_2:	A set of demand points where recharging is not possible
U:	A set of different scenarios

Parameters

Parameters	**Description**
r_i:	The amount of delivery demand of demand points i
P_i:	The amount of pickup demand of demand points i
S_i:	Time to provide service to demand points i
Q_k:	Loading capacity of each RPA k
a_i:	The earliest time allowed to provide service to distributor i in the hard time window
b_i:	The latest time allowed to provide service to distributor i in the hard time window
M:	Optional large number
ES_i:	The earliest time allowed to provide service to distributor i in the soft time window
LS_i:	The latest time allowed to provide service to distributor i in the soft time window
W_2:	Cost per unit time deviation from the earliest time allowed in the soft time window
W_3:	Cost per unit time deviation from the latest time allowed in the soft time window
fix'_k:	Fixed cost of using RPA k
C:	Cost of one charging unit
AT:	Minimum amount of charging allowed inside the RPA
Cf_f:	Preparing cost of a unit in facility location f
fix_d:	Cost of constructing distributor candidate location d
TS_i:	Time to provide service to demand point i
DAY:	The length of a working day
cp_{ji}:	RPA battery consumption from node i to node j
dx_{ij}:	The distance between node i and node j
full:	Battery charging capacity
p_u:	The probability of occurrence of scenarios u
V_{ku}:	The velocity of RPA k in event u
cap_d:	The capacity of candidate location of distributor d
$\overline{cap}_f$:	The capacity of facility location f
$L0_k$:	The load on RPA k when leaving the distributor
S_{ij}^k :	The risk of route deriving from node i to node j with RPA k
x_{ijkd}:	The variables zero and one. If RPA $k \in K$ belonging to candidate distributor locations d travels from node i to node j, it is equal to one and otherwise zero
s_{iu}:	The time to start providing service to demand point i in scenario u
L_j:	The weight of the load remaining on the RPA after service to demand point j
Z_d	The variables zero and one. If distributor d is constructed, it is equal to one and otherwise zero
E_{iu}:	The time deviation from the earliest time allowed to provide service to demand point i in the soft time window in scenario u
L_{iu}:	The time deviation from the latest time allowed to provide service to demand point i in the soft time window in scenario u
FC_k	The time to end the route of RPA k
de_d	The center demand of distributor d
Y_{df}	Variables zero and one. If distributor d is assigned to facility location f, it is equal to one and otherwise zero
A_i:	The amount of battery available on the RPA

References

1. Joerss, M.; Schroder, J.; Neuhaus, F.; Klink, C.; Mann, F. *Parcel Delivery: The Future of Last Mile*; Mckinsey & Company: London, UK, 2016.
2. Karak, A.; Abdelghany, K. The hybrid vehicle-drone routing problem for pick-up and delivery services. *Transp. Res. Part C* **2019**, *102*, 427–449. [CrossRef]
3. Peng, K.; Liu, W.; Sun, Q.; Ma, X.; Hu, M.; Wang, D.; Liu, J. Wide-Area Vehicle-Drone Cooperative Sensing: Opportunities and Approaches. *IEEE Access* **2019**, *7*, 1818–1828. [CrossRef]
4. Dawaliby, S.; Aberkane, A.; Bradai, A. Blockchain-based IoT platform for autonomous drone operations management. In Proceedings of the 2nd ACM MobiCom Workshop on Drone Assisted Wireless Communications for 5G and Beyond, London, UK, 25 September 2020.
5. Xiang, G.; Hardy, A.; Rajeh, M.; Venuthurupalli, L. Design of the life-ring drone delivery system for rip current rescue. In Proceedings of the 2016 IEEE Systems and Information Engineering Design Symposium (SIEDS), Charlottesville, VA, USA, 29 April 2016; pp. 181–186.
6. Albornoz, C.; Giraldo, L.F. Trajectory design for efficient crop irrigation with a UAV. In Proceedings of the 2017 IEEE 3rd Colombian Conference on Automatic Control (CCAC), Cartagena, Colombia, 18–20 October 2017; pp. 1–6.
7. Troudi, A.; Addouche, S.-A.; Dellagi, S.; El Mhamedi, A. Logistics Support Approach for Drone Delivery Fleet. In Proceedings of the 14th International Conference on Smart Cities, Málaga, Spain, 11–12 November 2017; pp. 86–96. [CrossRef]
8. Kunze, O. Replicators, Ground Drones and Crowd Logistics A Vision of Urban Logistics in the Year 2030. *Transp. Res. Procedia* **2016**, *19*, 286–299. [CrossRef]
9. Menouar, H.; Guvenc, I.; Akkaya, K.; Uluagac, A.S.; Kadri, A.; Tuncer, A. UAV-enabled intelligent transportation systems for the smart city: Applications and challenges. *IEEE Commun. Mag.* **2017**, *55*, 22–28. [CrossRef]
10. Dehin, G.; Zanetti, M.; de Araújo, O.; Cardoso, G., Jr. Minimizing dispersion in multiple drone routing, Computer and operation research. *Comput. Oper. Res.* **2019**, *109*, 28–42. [CrossRef]
11. Alfeo Mario, A.L.; Cimino, G.C.A.; Vaglini, G. Enhancing biologically inspired swarm behavior: Metaheuristics to foster the optimization of UAVs coordination in target search. *Comput. Oper. Res.* **2019**, *110*, 34–47. [CrossRef]
12. Hu, X.; Pang, B.; Dai, F.; Low, K.H. Risk Assessment Model for UAV Cost-Effective Path Planning in Urban Environments. *IEEE Access* **2020**, *8*, 150162–150173. [CrossRef]
13. Guerriero, F.; Surace, R.; Loscrí, V.; Natalizio, E.A. Multi-objective approach for unmanned aerial vehicle routing problem with soft time windows constraints. *Appl. Math. Model.* **2014**, *38*, 839–852. [CrossRef]
14. Doole, M.; Ellerbroek, J.; Hoekstra, J. Estimation of traffic density from drone-based delivery in very low level urban airspace. *J. Air Transp. Manag.* **2020**, *88*, 101862. [CrossRef]
15. Janik, P.; Zawistowski, M.; Fellner, R.; Zawistowski, G. Unmanned Aircraft Systems Risk Assessment Based on SORA for First Responders and Disaster Management. *Appl. Sci.* **2021**, *11*, 5364. [CrossRef]
16. Chauhan, D.R.; Unnikrishnan, A.; Figliozzi, M.; Boyles, S.D. Robust Maximum Coverage Facility Location Problem with Drones Considering Uncertainties in Battery Availability and Consumption. *Transp. Res. Rec.* **2021**, *2675*, 25–39. [CrossRef]
17. Chauhan, D.; Unnikrishnan, A.; Figliozzi, M. Maximum Coverage Capacitated Facility Location Problem with Range Constrained Drones. *Transp. Res. Part C Emerg. Technol.* **2019**, *99*, 1–18. [CrossRef]
18. Park, H.; Son, D.; Koo, B.; Jeong, B. Waiting strategy for the vehicle routing problem with simultaneous pickup and delivery using genetic algorithm. *Expert Syst. Appl.* **2020**, *165*, 113959. [CrossRef]
19. Ohmori, S.; Yoshimoto, K. Multi-product multi-vehicle inventory routing problem with vehicle compatibility and site dependency: A case study in the restaurant chain industry. *Uncertain Supply Chain Manag.* **2021**, *9*, 351–362. [CrossRef]
20. Khoufi, I.; Laouiti, A.; Adjih, C.; Hadded, M. UAVs Trajectory Optimization for Data Pick Up and Delivery with Time Window. *Drones* **2021**, *5*, 27. [CrossRef]
21. Choi, Y.; Schonfeld, P.M. Drone Deliveries Optimization with Battery Energy Constraints. In Proceedings of the Transportation Research Board 97th Annual Meeting, Washington, DC, USA, 7–11 January 2018.
22. Allouch, A.; Koubaa, A.; Khalgui, M.; Abbes, T. Qualitative and Quantitative Risk Analysis and Safety Assessment of Unmanned Aerial Vehicles Missions Over the Internet. *IEEE Access* **2019**, *7*, 53392–53410. [CrossRef]
23. Wang, S.; Na, J.; Xing, Y. Adaptive optimal parameter estimation and control of servo mechanisms: Theory and experiments. *IEEE Trans. Ind. Electron.* **2020**, *68*, 598–608. [CrossRef]
24. Sanz, D.; Valente, J.; del Cerro, J.; Colorado, J.; Barrientos, A. Safe operation of mini UAVs: A review of regulation and best practices. *Adv. Robot.* **2015**, *29*, 1221–1233. [CrossRef]
25. Wu, G.; Zhao, K.; Cheng, J.; Ma, M. A Coordinated Vehicle–Drone Arc Routing Approach Based on Improved Adaptive Large Neighborhood Search. *Sensors* **2022**, *22*, 3702. [CrossRef]
26. Barmpounakis, E.N.; Vlahogianni, E.I.; Golias, J.C. Unmanned Aerial Aircraft Systems for transportation engineering: Current practice and future challenges. *Int. J. Transp. Sci. Technol.* **2016**, *5*, 111–122. [CrossRef]
27. Marinelli, M.; Caggiani, L.; Ottomanelli, M.; Dell'Orco, M. En route truck–drone parcel delivery for optimal vehicle routing strategies. *IET Intell. Transp. Syst.* **2018**, *12*, 253–261. [CrossRef]
28. Coutinho, W.P.; Battarra, M.; Fliege, J. The unmanned aerial vehicle routing and trajectory optimization problem, a taxonomic review. *Comput. Ind. Eng.* **2018**, *120*, 116–128. [CrossRef]

29. Cheng, C.; Adulyasak, Y.; Rousseau, L.M.; Sim, M. Robust Drone Delivery with Weather Information, optimization online, internet database. *History* **2019**, 1–37. Available online: www.optimization-online.org/DB_FILE/2020/07/7897.pdf (accessed on 15 April 2022).
30. Rojas Viloria, D.; Solano-Charris, E.L.; Muñoz-Villamizar, A.; Montoya-Torres, J.R. Unmanned aerial vehicles/drones in vehicle routing problems: A literature review. *Int. Trans. Oper. Res.* **2021**, *28*, 1626–1657. [CrossRef]
31. Macrina, G.; Di Puglia Pugliese, L.; Guerriero, F.; Laporte, G. Drone-aided routing: A literature review. *Transp. Res. Part C Emerg. Technol.* **2020**, *120*, 102762. [CrossRef]
32. Poikonen, S.; Campbell, J.F. Future directions in drone routing research. *Networks* **2021**, *77*, 116–126. [CrossRef]
33. Kitjacharoenchai, P.; Min, B.; Lee, S. Two echelon vehicle routing problem with drones in last mile delivery. *Int. J. Prod. Econ.* **2020**, *225*, 107598. [CrossRef]
34. Kuo, R.; Lu, S.-H.; Lai, P.-Y.; Mara, S.T.W. Vehicle routing problem with drones considering time windows. *Expert Syst. Appl.* **2022**, *191*, 116264. [CrossRef]
35. Ribeiro, R.G.; Junior, J.R.C.; Cota, L.P.; Euzebio, T.A.M.; Guimaraes, F.G. Unmanned Aerial Vehicle Location Routing Problem with Charging Stations for Belt Conveyor Inspection System in the Mining Industry. *IEEE Trans. Intell. Transp. Syst.* **2020**, *21*, 4186–4195. [CrossRef]
36. Lin, X.; Wang, C.; Wang, K.; Li, M.; Yu, X. Trajectory planning for unmanned aerial vehicles in complicated urban environments: A control network approach. *Transp. Res. Part C Emerg. Technol.* **2021**, *128*, 103120. [CrossRef]
37. Gunawardena, N.; Leang, K.K.; Pardyjak, E. Particle swarm optimization for source localization in realistic complex urban environments. *Atmos. Environ.* **2021**, *262*, 118636. [CrossRef]
38. Lynskey, J.; Thar, K.; Oo, T.Z.; Hong, C.S. Facility Location Problem Approach for Distributed Drones. *Symmetry* **2019**, *11*, 118. [CrossRef]
39. Faiz, T.I.; Vogiatzis, C.; Noor-E-Alam, M. Robust Two-Echelon Vehicle and Drone Routing for Post Disaster Humanitarian Operations. *arXiv* **2020**, arXiv:2001.06456.
40. Shahzaad, B.; Bouguettaya, A.; Mistry, S. Robust Composition of Drone Delivery Services under Uncertainty. In Proceedings of the 2021 IEEE International Conference on Web Services (ICWS), Chicago, IL, USA, 5–10 September 2021; pp. 675–680.
41. Pugliese, L.D.P.; Guerriero, F.; Scutellá, M.G. The Last-Mile Delivery Process with Trucks and Drones Under Uncertain Energy Consumption. *J. Optimum. Theory Appl.* **2021**, *191*, 31–67. [CrossRef]
42. Kim, S.J.; Lim, G.J.; Cho, J. A Robust Optimization Approach for Scheduling Drones Considering Uncertainty of Battery Duration. *Comput. Ind. Eng.* **2018**, *117*, 291–302. [CrossRef]
43. Corbetta, M.; Kulkarni, C.S. An approach for uncertainty quantification and management of Unmanned aerial vehicle health. In Proceedings of the 2019 Annual Conference of the Prognostics and Health Management Society, Scottsdale, AZ, USA, 21–26 September 2019.
44. Sawadsitang, S.; Niyato, D.; Tan, P.S.; Wang, P.; Nutanong, S. Multi-Objective Optimization for Drone Delivery. In Proceedings of the 2019 IEEE 90th Vehicular Technology Conference, Honolulu, HI, USA, 22–25 September 2019; pp. 1–5.
45. Ilić, D.; Milošević, I.; Ilić-Kosanović, T. Application of Unmanned Aircraft Systems for smart city transformation: Case study Belgrade. *Technol. Forecast. Soc. Chang.* **2022**, *176*, 121487. [CrossRef]
46. Bertrand, S.; Raballand, N.; Viguier, F. Evaluating Ground Risk for Road Networks Induced by UAV Operations. In Proceedings of the 2018 International Conference on Unmanned Aircraft Systems (ICUAS), Dallas, TX, USA, 12–15 June 2018; pp. 168–176.
47. Aminbakhsh, S.; Gunduz, M.; Sonmez, R. Safety risk assessment using analytic hierarchy process (AHP) during planning and budgeting of construction projects. *J. Saf. Res.* **2013**, *46*, 99–105. [CrossRef] [PubMed]
48. Shao, P.-C. Risk Assessment for UAS Logistic Delivery under UAS Traffic Management Environment. *Aerospace* **2022**, *7*, 140. [CrossRef]
49. Denney, E.; Pai, G.; Johnson, M. Towards a Rigorous Basis for Specific Operations Risk Assessment of UAS. In Proceedings of the 2018 IEEE/AIAA 37th Digital Avionics Systems Conference (DASC), London, UK, 23–27 September 2018; pp. 1–10.
50. Capitán, C.; Jesús, C.; Castaño, Á.R.; Ollero, A. Risk Assessment based on SORA Methodology for a UAS Media Production Application. In Proceedings of the 2019 International Conference on Unmanned Aircraft Systems (ICUAS), Atlanta, GA, USA, 11–14 June 2019; pp. 451–459.
51. Mulvey, J.M.; Vanderbei, R.J.; Zenios, S.A. Robust Optimization of Large-Scale Systems. *Oper. Res.* **1995**, *43*, 264–281. [CrossRef]
52. Erkut, E.; Ingolfsson, A. Transport risk models for hazardous materials: Revisited. *Oper. Res. Lett.* **2005**, *33*, 81–89. [CrossRef]
53. JARUS Guidelines on Specific Operations Risk Assessment (SORA). 2021. Available online: http://jarus-rpas.org/sites/jaruspas.org/files/jar_doc_06_jarus_sora_v2.0.pdf (accessed on 15 April 2022).
54. Deb, K.; Goel, T. Controlled Elitist Non-dominated Sorting Genetic Algorithms for Better Convergence. In Proceedings of the International Conference on Evolutionary Multi-Criterion Optimization, Ouro Preto, Brazil, 5–8 April 2001; Volume 1993, pp. 67–81.
55. Ren, X.; Cheng, C. Model of Third-Party Risk Index for Unmanned Aerial Vehicle Delivery in Urban Environment. *Sustainability* **2020**, *12*, 8318. [CrossRef]
56. Aykut, T. Determination of groundwater potential zones using Geographical Information Systems (GIS) and Analytic Hierarchy Process (AHP) between Edirne-Kalkansogut (northwestern Turkey). *Groundw. Sustain. Dev.* **2021**, *12*, 100545. [CrossRef]

57. Zhang, Y.; Zhan, Y.L.; Tan, Q.M. Studies on human factors in marine engine accident. In Proceedings of the Second International Symposium on Knowledge Acquisition and Modeling: KAM, Wuhan, China, 30 November 2009; Volume 1, pp. 134–137.
58. Kahn, K.B.; Kay, S.E.; Slotegraaf, R.J.; Urban, S. *PDMA Handbook of New Product Development*, 3rd ed.; John Wiley & Sons: Hoboken, NY, USA, 2013.
59. Saaty, T.L. How to make a decision—the analytic hierarchy process. *Eur. J. Oper. Res.* **1990**, *48*, 9–26. [CrossRef]